UNIVERSITY OF LEEDS

This is a repository copy of *Design and modelling of a compliant ankle rehabilitation robot redundantly driven by pneumatic muscles*.

White Rose Research Online URL for this paper:
http://eprints.whiterose.ac.uk/154168/

Version: Accepted Version

Proceedings Paper:
Meng, W orcid.org/0000-0003-0209-8753, Zhu, C, Zuo, J et al. (3 more authors) (2019) Design and modelling of a compliant ankle rehabilitation robot redundantly driven by pneumatic muscles. In: 2019 IEEE/ASME International Conference on Advanced Intelligent Mechatronics (AIM). IEEE/ASME International Conference on Advanced Intelligent Mechatronics, AIM, 08-12 Jul 2019, Hong Kong. IEEE , pp. 459-464. ISBN 9781728124933

https://doi.org/10.1109/AIM.2019.8868903

©2019 IEEE. Personal use of this material is permitted. Permission from IEEE must be obtained for all other uses, in any current or future media, including reprinting/republishing this material for advertising or promotional purposes, creating new collective works, for resale or redistribution to servers or lists, or reuse of any copyrighted component of this work in other works.

Reuse
Items deposited in White Rose Research Online are protected by copyright, with all rights reserved unless indicated otherwise. They may be downloaded and/or printed for private study, or other acts as permitted by national copyright laws. The publisher or other rights holders may allow further reproduction and re-use of the full text version. This is indicated by the licence information on the White Rose Research Online record for the item.

Takedown
If you consider content in White Rose Research Online to be in breach of UK law, please notify us by emailing eprints@whiterose.ac.uk including the URL of the record and the reason for the withdrawal request.

White Rose
university consortium
Universities of Leeds, Sheffield & York

eprints@whiterose.ac.uk
https://eprints.whiterose.ac.uk/

Design and Modelling of a Compliant Ankle Rehabilitation Robot Redundantly Driven by Pneumatic Muscles*

Wei Meng, *Member, IEEE,* Chengxiang Zhu, Jie Zuo, Qingsong Ai, Quan Liu, Sheng Q. Xie, *Senior Member, IEEE*

***Abstract*— Ankle sprains are the most common type of ankle injuries for the general public. Due to the lack of human manual therapy resources, it is highly demanding for robot-assisted rehabilitation training. However, most of the current robotic ankle rehab devices are driven by rigid actuators and have problems such as limited degrees of freedom, lack of safety and compliance and poor flexibility. This paper will design a new version of compliant ankle rehabilitation robot redundantly driven by pneumatic muscles (PMs) to provide full range of motion and torque ability for human ankle with enhanced safety and adaptability, attributing to the PM's high power/mass ratio, good flexibility and light weight advantages. In this paper, the driving characteristics of the PM actuators, as well as the kinematics and rehabilitation requirements of the ankle joint are analyzed. A new type of ankle rehabilitation robot that is redundantly driven by five PMs is designed and modeled. The ankle joint can be compliantly driven by the robot with full three degrees of freedom to perform dorsiflexion/plantarflexion, inversion/ eversion and adduction/abduction training. Then the kinematics and dynamics model of the rehabilitation robot is established to validate and verify the design and the models.**

I. INTRODUCTION

Globally, 15M people suffer a stroke every year, causing 5M permanently disabled, which makes stroke the second leading cause of disability [1]. Ankle sprains, which involve overstretching the ligaments and soft tissues around the ankle, are the most common type of ankle injuries. In the UK, there are >2 million emergency department visits with sprained ankles a year, accounting for 5,600 incidences per day [2]. In sports, ankle injuries are the most frequent injuries with ankle sprains accounting for 76.7% of total ankle injuries [3]. They have the highest incidence rate among various sports, i.e. the rates are 100%, 23.3%, and 17.4% for field hockey, rugby and basketball, respectively [3]. The economic burden of ankle sprains is significant and the average cost of treating ankle sprain is approximately £940 [4], amounting to an estimated annual direct treatment cost of > £2 billion. The total indirect costs, e.g. costs of travel, productivity loss and medical treatment, will exceed £12 billion each year, imposing tremendous economic burden on the UK society [5].

It is widely accepted that the development of chronic ankle instability is dependent upon the interaction of various mechanical and sensorimotor functional instabilities; therefore ankle rehabilitation, which aims to restore the ankle ability so that is can move with a full range of motion, enhance the muscle strength, and improve the proprioception control, is required to prevent progression of a single acute ankle sprain event into a chronically unstable condition [6]. The repetitive and tedious nature of rehabilitation makes the use of a robotic system an attractive alternative for ankle treatment. Our review shows that limitations exist in current robots, such as the inappropriate robotic design, small range of motion (RoM) and limited force/torque capability [7]. Meanwhile, most of the current ankle rehabilitation robots are driven by rigid actuators, which have problems such as lack of safety and poor flexibility. There are a few preliminary robotic prototypes for post-stroke rehabilitation, but no robotic devices developed specifically for ankle sprain assessment and treatment [8]. For example, MIT Anklebot [9] and Robotic Gait Trainer [10] can only operate with a single degree of freedom (DoF). Existing multiple DoFs ankle robots such as Rutgers Ankle [11] and ARBOT [12] are driven by rigid and stiff actuators [13]. Ankle sprains have physical damage to ankle ligaments and tissues which lead to mechanical and functional instabilities [14]. The mechanical structure requirement, medical fundamentals, assessment and treatment of patients with ankle sprains raise challenges in the design of compliant ankle robot.

Pneumatic muscles (PMs) have the characteristics of high output/self-weight ratio and are therefore suitable for wearable and rehabilitation robots when interacting with humans. As PM can only provide pulling force rather than pushing force, two pneumatic muscles are usually adopted in an antagonist structure to realize the rotary motion of a single joint. Huang et al. [15] designed a 2-DoF wrist rehabilitation robot driven by two pairs of pneumatic muscles with a pulley to achieve the rotation of the wrist joint. Cao et al. [16] designed a knee exoskeleton robot using four pneumatic muscles to achieve flexion and extension of the knee joint in the form of antagonistic pairs and pulleys. For single DoF joints such as hip or knee, the antagonistic structure is competent. However, for joints with multiple DoFs such as the ankle joint, the large-scope use of the antagonistic modules will significantly increase the mechanical complexity and control. Parallel mechanism has the advantages of strong loading capacity and small operation error, and is suitable for the rehabilitation of ankle joints [17]. A parallel ankle rehabilitation robot actuated

---

*Research supported by National Natural Science Foundation of China under grant numbers 51705381 and 51675389 and the Natural Science Foundation of Hubei Province (2017CFB428).

W. Meng is with the School of Information Engineering, Wuhan University of Technology, 122 Luoshi Road, Wuhan, China and the School of Electronic and Electrical Engineering, University of Leeds, Leeds, LS2 9JT, UK (email: weimeng@whut.edu.cn, w.meng@leeds.ac.uk).

C. Zhu is with School of Information Engineering, Wuhan University of Technology, 122 Luoshi Road, Wuhan, China (zchengx0508@whut.edu.cn).

J. Zuo is with the School of Information Engineering, Wuhan University of Technology, 122 Luoshi Road, Wuhan, China (zuojie@whut.edu.cn).

Q. Ai is with the School of Information Engineering, Wuhan University of Technology, 122 Luoshi Road, Wuhan, China (qingsongai@whut.edu.cn).

Q. Liu is with the School of Information Engineering, Wuhan University of Technology, 122 Luoshi Road, Wuhan, China (quanliu@whut.edu.cn).

S. Q. Xie is with the School of Electronic and Electrical Engineering, University of Leeds, Leeds, LS2 9JT, UK (email: s.q.xie@leeds.ac.uk).

by PMs has been developed by the University of Auckland [18], it employs four parallel PMs to actuate the user's ankle joint [19]. The robot consists of two parallel platforms, a fixed platform and a moving platform that is actuated by four PMs in parallel. An updated version with more powerful Festo muscles and three-link lower platform to regulate the ankle three DoFs were further developed and tested [20, 21]. This design allows the participant's lower limb and shinbone to stay stationary during the ankle training process. However, limitations still exist for these parallel robots. Due to the strict symmetry of the four muscles, the torque ability and RoM of the robot in adduction/abduction is quite week. As the PM can only provide unidirectional force, it is essential to add a redundant actuation to achieve the required movements.

In this paper, a new type of parallel ankle rehabilitation robot redundantly driven by PMs with full three-DoF and RoM abilities will be designed and modeled. The rest of this paper is organized as follows: Section II analyzes the human ankle motion features and designs the mechanical structure and components. The robot kinematic and dynamic models will be established in Section III to validate the mechanism design. In Section IV, we perform simulations to verify the robot movement ability by comparing experimental results. Conclusion and future work are presented finally.

II. ANKLE MOTION AND ROBOT DESIGN

A. *Ankle Movement Features*

As one of the most complicated structures of the human body, the ankle is also very vulnerable. To appropriately deliver ankle rehabilitation, the designed robot structure must consider the ankle movement features and meet the training needs. Human ankle is mainly composed of the ankle joint and the talus joint, as shown in Fig. 1(a). The ankle joint is mainly composed of the lower end of the humerus, the tibia and the talus, while the talus joint mainly includes the talus and the calcaneus. In this paper, the ankle joint will be treated as a three-DoF revolute joint, as shown in Fig. 2(b), i.e., the three rotational DoFs are the dorsiflexion/plantarflexion around the X axis, the inversion/eversion around the Y axis, and the adduction/abduction rotation around the Z axis.

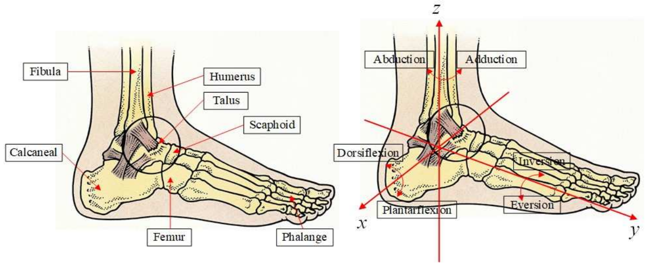

Figure 1. Analysis of the ankle movement: (a) bilogical structure of the ankle (b) ankle moving degrees of freedom

In order to design a robot meeting the rehabilitation needs of the ankle, it is necessary to realize the rotational movement of the ankle in the three DoFs around the X, Y and Z axes, especially the rotational RoM which plays a major role [22]. Table 1 shows the maximum RoM of the ankle. The robot must have a workspace that covers the typical range of motion of the human ankle in most situations, in order to carry out different ankle rehabilitation exercises easily.

TABLE I. RANGE OF MOTION OF THE HUMAN ANKLE

	Ankle Motions	**Maximum RoM**
$+\theta_x$	Dorsiflexion	20.3°-29.8°
$-\theta_x$	Plantarflexion	32.6°-40.8°
$+\theta_y$	Inversion	14.5°-22.0°
$-\theta_y$	Eversion	10.0°-17.0°
$+\theta_z$	Adduction	22.0°-36.0°
$-\theta_z$	Abduction	15.4°-25.9°

B. *Robot Mechanism Design*

As pneumatic muscles can only provide tension force, there must be a redundancy to achieve force closure of the robot. That is, to complete a rotational motion of degrees of freedom, at least a pneumatic muscle actuator is required [23]. Many parallel ankle rehabilitation devices are driven from the downside with the upper platform constrained about a center of rotation which is usually not coincident with the actual ankle center. In order to meet the above-mentioned RoM and rehabilitation needs of the ankle, this paper designs a rehabilitation robot with the driving part on the top and the moving platform below, which can ensure the rotation center of the robot is in consistent with the rotation center of the participant's ankle. The design is actuated from the top and thus enable the user to wear it with the shank be stationary.

The designed ankle robot is mainly composed of a moving platform, a driving module and a support module to help the patient complete three ankle rotational movements, while the translation in the three directions of X, Y, and Z axes can be restricted. The moving platform model is shown in Fig. 2, which includes the rotating platform joint 1 (X-axis) and its left and right support rods, the rotating platform joint 2 (Y-axis) and the rotating platform joint 3 (Z-axis). The robot will be equipped with foot plate, angle sensors and six-axis force/torque sensor to monitor the robot movement as well as the human robot interaction. The left and right shaft supports are fixed on the base. Joint 1 support is connected to joint 1 through the rotating shaft and the deep groove ball bearing. Joint 1 is also connected with the crankshaft of joint 2, and the crankshaft of joint 2 is connected with the moving platform through the joint 3 and the thrust ball bearing. Finally, the moving platform is connected with the foot pedal.

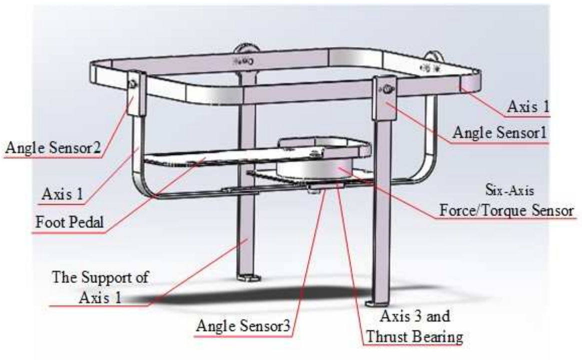

Figure 2. Moving platform of the designed robot

The robot driving module is shown in Fig. 3, which mainly includes pneumatic muscle components, pulley brackets, fixed pulleys and swingable pulleys. PM1 and PM2 are connected to the fixed point of the front end of the moving platform by the wire rope through the swinging pulleys. The moving platform will be driven rotating around the Y-axis to reach ankle inversion/eversion when PM1 or PM2 is contracted. PM3 and PM4 are connected to the front end of the moving platform by the wire rope through the swinging pulleys. Similarly, the moving platform will be driven rotating around the Z-axis to reach ankle adduction/abduction when PM3 or PM4 is contracted. PM5 is connected to the back end of the moving platform by the two fixed pulleys and the swinging pulley by a steel rope. When PM5 or PM1 and PM2 are contracted, the moving platform is rotated about the X-axis to help the ankle joint perform dorsiflexion/plantarflexion movement.

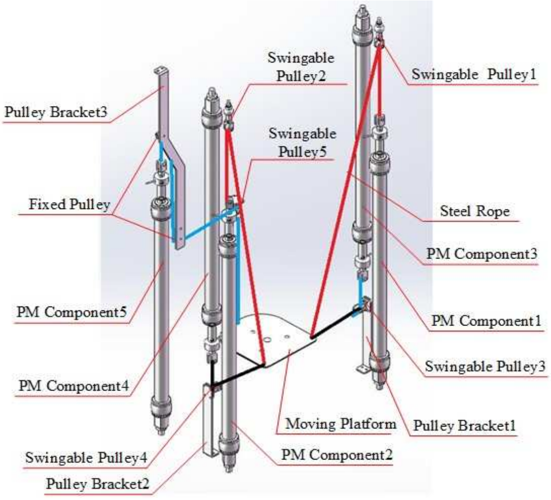
Swingable Pulley2
Swingable Pulley1
Pulley Bracket3
Swingable Pulley5
Fixed Pulley
Steel Rope
PM Component3
PM Component5
PM Component1
Swingable Pulley3
PM Component4
Moving Platform
Pulley Bracket1
Swingable Pulley4
PM Component2
Pulley Bracket2

Figure 3. Driving module of the designed robot

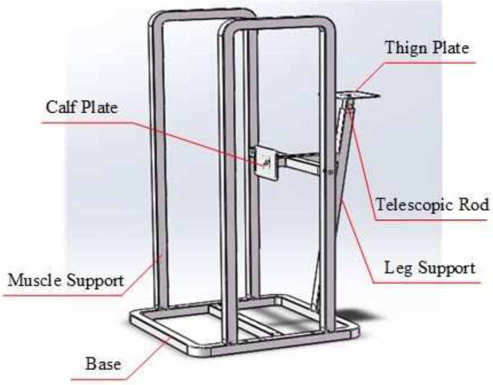
Thign Plate
Calf Plate
Telescopic Rod
Leg Support
Muscle Support
Base

Figure 4. Support structure of the designed robot

The support structure is shown in Fig. 4. It mainly includes the base, muscle support, leg support and lower limb support. The muscle support and the leg support are bolted to the base. The thigh plate and the calf plate are bolted to the leg rests. The telescopic rod is used to adjust the height of the thigh plate to meet the requirements of patients with different leg lengths. The telescopic rod is fixed on the leg support rod by the positioning pin and the guide bolt, and the positioning pin is used for positioning and adjusting the height. The rail bolts are used to limit the extent to which the telescopic rod is pulled out of the leg rests. One side of the telescopic rod has a rail groove with a vertical height of 89 mm, and the other side has ten positioning holes, and the spacing of the positioning holes is 9.9 mm. The adjustable vertical height of the telescopic rod is 89mm, and the adjustment range is divided into 9 levels, each of which can be increased by 9.9mm.

III. KINEMATICS AND DYNAMICS MODELLING

A. Kinematics Modelling

Inverse kinematics of robot describes the relationship between the rotation angle of the moving platform and the displacement of each link as well as the PM actuator, which is the basis for position control of the ankle rehabilitation robot. Geometric model of the designed robot is shown in Fig. 5. The coordinate system of upper platform is defined as $O_f - XYZ$, the coordinate system of lower moving platform is $O_m - XYZ$, actual rotating coordinate system of the moving platform is $O_R - XYZ$, $P_i^f\ (i = 1, 2, \cdots, 5)$ represent the connection points of the cable with the fixed platform, while the connection points with the moving platform are represented by $P_i^m\ (i = 1, 2, \cdots, 5)$. The distance between the fixed platform center O_f and the rotating center of the moving platform O_R is $H = 0.477m$. The distance between the actual rotating center O_R and the geometric center of the moving platform O_m is $h = 0.106m$. The coordinates of P_i^f and P_i^m in their respective coordinate systems are illustrated in (1) and (2).

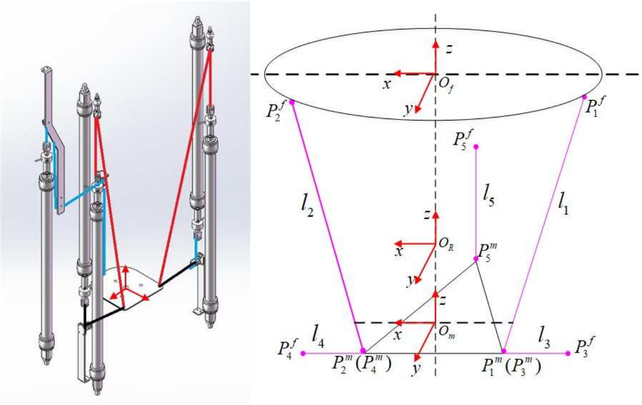
z
x
O_f
y
P_2^f
P_1^f
P_5^f
l_2
l_5
l_1
z
x
O_R
P_5^m
y
z
x
O_m
l_4
l_3
P_4^f
P_3^f
$P_2^m(P_4^m)$
y
$P_1^m(P_3^m)$

Figure 5. Mechanism and geometric model of the ankle robot

$$
\begin{aligned}
P_1^f &= [-0.1875\ \ 0.089\ \ 0]^T \\
P_2^f &= [0.1875\ \ 0.089\ \ 0]^T \\
P_3^f &= [-0.1725\ \ 0.05\ \ -0.583]^T \\
P_4^f &= [0.1725\ \ 0.05\ \ -0.583]^T \\
P_5^f &= [0\ \ -0.074\ \ -0.345]^T
\end{aligned} \tag{1}
$$

$$
\begin{aligned}
P_1^m &= P_3^m = [-0.06\ \ 0.05\ \ \text{-}0.106]^T \\
P_2^m &= P_4^m = [0.06\ \ 0.05\ \ \text{-}0.106]^T \\
P_5^m &= [0\ \ -0.074\ \ -0.106]^T
\end{aligned} \tag{2}
$$

Defining rotational angle vector of the moving platform as $\boldsymbol{q} = [\theta_x\ \ \theta_y\ \ \theta_z]^T$, where θ_x, θ_y and θ_z represent the rotation angle of the moving platform around the X, Y, and Z axis.

$$\overrightarrow{O_f O_R} = [0\ \ 0\ \ -H]^T \tag{3}$$

According to the geometric model shown in Fig. 5, the displacement vector of the i^{th} link can be expressed as:

$$\boldsymbol{L}_i = \overrightarrow{O_f O_R} + \boldsymbol{R}\overrightarrow{O_R P_i^m} - \overrightarrow{O_f P_i^f}\ \left(i=1,2,\cdots,5\right) \tag{4}$$

where $\overrightarrow{O_R P_i^m}$ is the position vector of P_i^m in the coordinate system $O_R - XYZ$, $\overrightarrow{O_f P_i^f}$ represents the position vector of P_i^f in the coordinate system $O_f - XYZ$, which are the inherent parameter information of the ankle rehabilitation robot, and they are independent of the robot lower platform movement. $\boldsymbol{R}$ is the rotation matrix of the robot moving platform, which is determined by the rotational angles of the moving platform $\boldsymbol{q}=[\theta_x \quad \theta_y \quad \theta_z]^T$. The rotation of the moving platform can be regarded as the rotation around the X axis, the Y axis and the Z axis respectively, wherein the rotation matrix around a single axis $\boldsymbol{R}_x$, $\boldsymbol{R}_y$ and $\boldsymbol{R}_z$ can be expressed as (5), then we can obtain the final rotation matrix $\boldsymbol{R}$ as in (6). In (5) and (6), *S* represents the *sin* () function and *C* represents the *cos* () function.

$$\boldsymbol{R}_x = \begin{bmatrix} 1 & 0 & 0 \\ 0 & C\theta_x & -S\theta_x \\ 0 & S\theta_x & C\theta_x \end{bmatrix},\ \boldsymbol{R}_y = \begin{bmatrix} C\theta_y & 0 & S\theta_y \\ 0 & 1 & 0 \\ -S\theta_y & 0 & C\theta_y \end{bmatrix}, \boldsymbol{R}_z = \begin{bmatrix} C\theta_z & -S\theta_z & 0 \\ S\theta_z & C\theta_z & 0 \\ 0 & 0 & 1 \end{bmatrix} \tag{5}$$

$$\boldsymbol{R}=\boldsymbol{R}_z\boldsymbol{R}_y\boldsymbol{R}_x = \begin{bmatrix} C\theta_y C\theta_z & -C\theta_x S\theta_z + S\theta_x S\theta_y C\theta_z & S\theta_x S\theta_z + C\theta_x S\theta_y C\theta_z \\ C\theta_y S\theta_z & C\theta_x C\theta_z + S\theta_x S\theta_y S\theta_z & -S\theta_x C\theta_z + C\theta_x S\theta_y S\theta_z \\ -S\theta_y & S\theta_x C\theta_y & C\theta_x C\theta_y \end{bmatrix} \tag{6}$$

Then the displacement change of each PM link is:

$$\Delta l_i = \left\|\boldsymbol{L}_i\right\| - l_{i0} = \left\|\overrightarrow{O_f O_R} + \boldsymbol{R}\overrightarrow{O_R P_i^m} - \overrightarrow{O_f P_i^f}\right\| - l_{i0}, (i=1,2,\cdots,5) \tag{7}$$

where l_{i0} is the initial length of the i^{th} link, in which $[l_{10}, l_{20}, l_{30}, l_{40}, l_{50}] = [598, 598, 112, 112, 238](mm)$. Each PM is 400mm long, so the total PM-cable length will be the sum of the two. If $\Delta l_i < 0$, it means that the PM needs to contract, Or $\Delta l_i > 0$ means that the PM needs to be stretched.

So far, the inverse kinematics model of the 3-DOF ankle rehabilitation robot has been established. Within the RoM of the ankle robot, the displacement of each PM actuator can be obtained using the inverse kinematics and the measured robot rotation angles. According to the displacement of all actuators, position control of the ankle robot can be realized.

B. Dynamics Modelling

Dynamics model of the robot describes the relationship between the expected output torque of the moving platform and the desired angles, velocities and accelerations. That is, to calculate how much torque is needed to drive the moving platform to reach the desired orientation. The moving platform of the designed ankle rehabilitation robot can be regarded as a 3-DOF serial robotic manipulator with three joint rotation axes. Therefore, the dynamics of the parallel robot can be established using the method of serial robot. Let the X-axis rotation axis be axis 1, the Y-axis rotation axis be axis 2, and the Z-axis rotation axis be axis 3. The model of the moving platform is illustrated as Fig. 6.

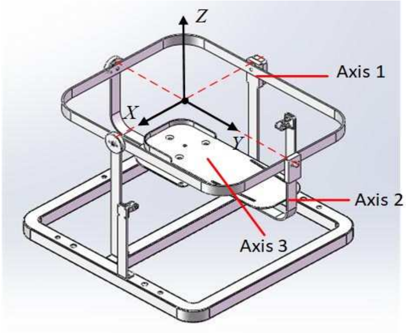

Figure 6. Moving platform of the ankle robot

Dynamics model of the robot is in form of:

$$\boldsymbol{M}(\boldsymbol{q})\ddot{\boldsymbol{q}} + \boldsymbol{C}(\boldsymbol{q},\dot{\boldsymbol{q}})\dot{\boldsymbol{q}} + \boldsymbol{G}(\boldsymbol{q}) = \boldsymbol{\tau} \tag{8}$$

where $\boldsymbol{M}(\boldsymbol{q})$ is the 3×3 inertia matrix of the robotic platform, $\boldsymbol{C}(\boldsymbol{q},\dot{\boldsymbol{q}})$ is a 3×3 matrix representing the centrifugal and Coriolis force of the robot platform. $\boldsymbol{G}(\boldsymbol{q})$ is the 3×1 gravity vector and $\boldsymbol{\tau}$ is the expected output torque of the robot.

$\boldsymbol{M}(\boldsymbol{q})$ can be expressed by (9):

$$\boldsymbol{M}(\boldsymbol{q}) = \begin{bmatrix} M_{11} & M_{12} & M_{13} \\ M_{21} & M_{22} & M_{23} \\ M_{31} & M_{32} & M_{33} \end{bmatrix} \tag{9}$$

where

$$M_{ij} = \sum_{p=\max(i,j)}^{3} Trace(\boldsymbol{U}_{pj}\boldsymbol{J}_p\boldsymbol{U}_{pi}^T) \tag{10}$$

$$\boldsymbol{U}_{ij} = \begin{cases} \boldsymbol{A}_1 \cdots \boldsymbol{A}_{j-1}\boldsymbol{Q}\boldsymbol{A}_j \cdots A_i & j \le i \\ 0 & j > i \end{cases} \tag{11}$$

$$\boldsymbol{Q} = \begin{bmatrix} 0 & -1 & 0 & 0 \\ 1 & 0 & 0 & 0 \\ 0 & 0 & 0 & 0 \\ 0 & 0 & 0 & 0 \end{bmatrix} \tag{12}$$

$\boldsymbol{J}_i$ is the pseudo-inertia matrix of the i^{th} axis, $\boldsymbol{A}_i$ is a homogeneous transformation matrix expressed as:

$$\boldsymbol{A}_i = \begin{bmatrix} \cos(\theta_i) & -\sin(\theta_i)\cos(\alpha_i) & \sin(\theta_i)\sin(\alpha_i) & 0 \\ \sin(\theta_i) & \cos(\theta_i)\cos(\alpha_i) & -\cos(\theta_i)\sin(\alpha_i) & 0 \\ 0 & \sin(\alpha_i) & \cos(\alpha_i) & 0 \\ 0 & 0 & 0 & 1 \end{bmatrix} \tag{13}$$

$\alpha_1 = \alpha_2 = \pi/2, \alpha_3 = 0, \theta_1 = \pi/2 + \theta_x, \theta_2 = \pi/2 + \theta_y$, $\theta_3 = \theta_z$.

$\boldsymbol{C}(q,\dot{q})$ can be expressed by (14):

$$\boldsymbol{C}(\boldsymbol{q},\dot{\boldsymbol{q}}) = \begin{bmatrix} \sum_{k=1}^{3} C_{11k}\dot{q}_k & \sum_{k=1}^{3} C_{12k}\dot{q}_k & \sum_{k=1}^{3} C_{13k}\dot{q}_k \\ \sum_{k=1}^{3} C_{21k}\dot{q}_k & \sum_{k=1}^{3} C_{22k}\dot{q}_k & \sum_{k=1}^{3} C_{23k}\dot{q}_k \\ \sum_{k=1}^{3} C_{31k}\dot{q}_k & \sum_{k=1}^{3} C_{32k}\dot{q}_k & \sum_{k=1}^{3} C_{33k}\dot{q}_k \end{bmatrix} \tag{14}$$

where

$$C_{ijk} = \sum_{p=\max(i,j,k)}^{3} Trace(\boldsymbol{U}_{pjk}\boldsymbol{J}_p\boldsymbol{U}_{pi}^T) \tag{15}$$

$$\boldsymbol{U}_{ijk} = \frac{\partial \boldsymbol{U}_{ij}}{\partial q_k} \tag{16}$$

$\boldsymbol{G}(\boldsymbol{q})$ can be expressed by (17):

$$\boldsymbol{G}(\boldsymbol{q}) = [G_1; G_2; G_3] \tag{17}$$

where

$$\begin{cases} G_1 = -m_1\boldsymbol{g}\boldsymbol{U}_{11}\boldsymbol{r}_1 - m_2\boldsymbol{g}\boldsymbol{U}_{21}\boldsymbol{r}_2 - m_3\boldsymbol{g}\boldsymbol{U}_{31}\boldsymbol{r}_3 \\ G_2 = -m_2\boldsymbol{g}\boldsymbol{U}_{22}\boldsymbol{r}_2 - m_3\boldsymbol{g}\boldsymbol{U}_{32}\boldsymbol{r}_3 \\ G_1 = -m_3\boldsymbol{g}\boldsymbol{U}_{33}\boldsymbol{r}_3 \end{cases} \tag{18}$$

IV. SIMULATION RESULTS AND DISCUSSION

Before development and integration of the robot in real life, MATLAB simulations were conducted to evaluate and verify the movement ability of the designed robot. The robot moving platform was controlled to track a predefined trajectory (sin wave trajectories with 30° amplitude in dorsiflexion/plantarflexion, 20° in inversion/ eversion and 25° in adduction/abduction, at 0.05 Hz frequency). By using inverse kinematics, the displacement of each PM link can be obtained as well as the velocity. Fig. 7 presents the simulation results of the robot kinematics model in terms of the desired rotation angles, the required PM link displacement, the resulted PM link change velocity and the calculated speed using Jacobian matrix.

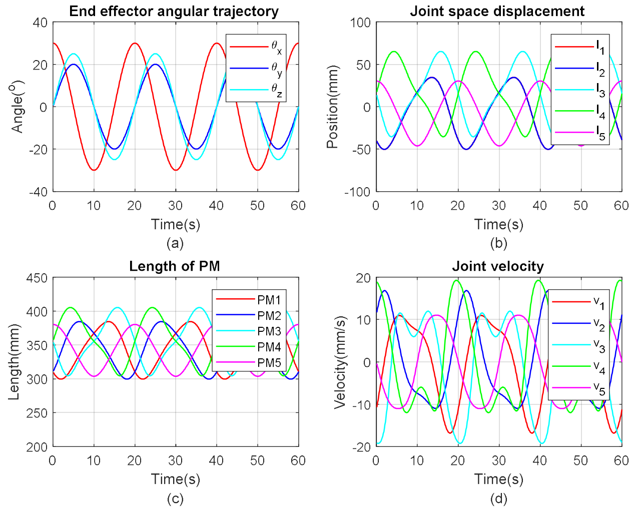

(a) (b) (c) (d)

Figure 7. Simulation results of the ankle robot kinematics model

Fig. 7(a) shows the desired rotation angles of the end moving platform, Fig. 7(b) is the displacement variation of each PM actuator obtained by using the inverse kinematics model. The length of each PM in free state is 400mm, while in the initial zero positon of the robot moving platform, all the PMs have to be inflated to the initial length, that is, [350, 350, 340, 340, 350]mm, Fig. 7(c) shows the change of each PM's length during the robot movement. Fig. 7(d) is the speed of each link obtained by using the Jacobian matrix. It can be seen that the robot moving platform is able to cover the full RoM of the human ankle and the kinematics model is validated.

The simulation results of the robot dynamics model are shown in Fig. 8, where Fig. 8(a) shows the desired motion trajectory of the moving platform. Fig. 8(b) shows the required output torque of the robot platform determined by the dynamic model. Fig. 8(c) is the gravity component of the robot model. It can be seen that the gravity component that robot needs to overcome is almost equal to the expected robot output torque, because in low-speed operation the inertia component, the centrifugal and Coriolis force component is small and almost negligible. To verify the dynamics model, Fig. 8(d) shows the pulling force of PM actuator obtained by using the Jacobian matrix. It can be seen that the obtained PM pulling force has a negative value, which means there will be a pushing force. As mentioned before, PM can only be contracted by inflation to provide pulling force, the negative force may lead to the loss of controllability. When integrating the robot system in real life, it is necessary to redistribute the pulling forces of PMs so that the driving force of each PM is refined greater than zero, ensuring the controllability and safety of the robot.

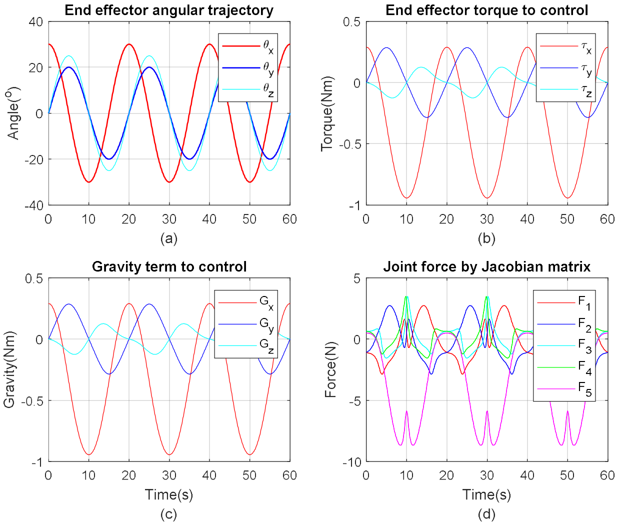

(a) (b) (c) (d)

Figure 8. Simulation results of the ankle robot dynamics model

This new version of robot is driven by five pneumatic muscles, connected to the moving platform by a flexible cable and using the pulley to change the direction of the driving force to achieve more movement DoFs of the ankle. From the simulation results, we can see that compared with the existing ankle rehabilitation robot driven by four pneumatic muscles such as [18] and [21], the robot can provide higher output torque and RoM for the human ankle, especially the rotation movement around Z-axis. As in Fig. 9, the RoM of each single dorsiflexion/plantarflexion, inversion/eversion and adduction/ abduction movement is easy to reach 35°, 25°, and 25°, with the PMs controlled under its contraction scope. In the case of four PMs-driven parallel robot, the driver is required to provide a horizontal pulling force when the moving platform rotates around the Z axis, in other words, the PM must change its driving force direction momentarily. In this way the rotational toque around Z-axis is too small to provide sufficient driving torque and range of motion for the ankle adduction/abduction movement. Moreover, when the moving platform rotates around the Z axis, if the drive is directly connected to the moving platform, they are easy to be twisted and this may easily damage the PM links. The ankle rehabilitation robot designed in this paper is able to significantly improve the horizontal driving force for the moving platform to rotate around Z axis. Compared with current ankle rehabilitation robot driven by four PMs, the designed robot costs a PM more, but it can provides much higher driving torque and range of motion in all freedoms.

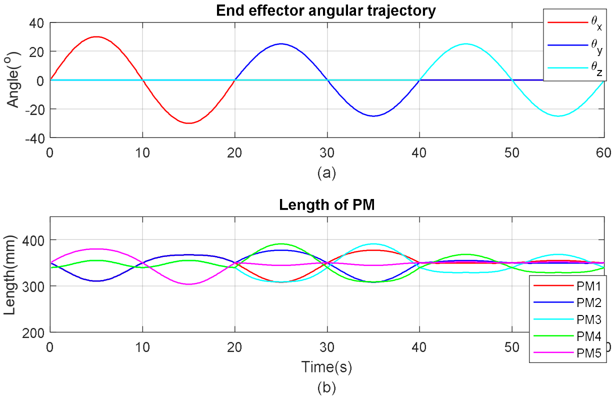

(a)

(b)

Figure 9. RoM of the ankle robot in three single movement

V. CONCLUSION

A new compliant ankle rehabilitation robot redundantly driven by five PMs was designed and modelled in this paper. By taking advantages of the PM's driving characteristics, this robot is able to provide higher output torque and full RoM for human ankle treatment. The kinematics and dynamics models of the robot are developed and simulation experiments were performed to validate the models and verity the robot moving ability. Results show that the robot can help the participant to reach large-scale movements in dorsiflexion/plantarflexion, inversion/eversion and especially in adduction/abduction, in which the maximum robot range of motion can definitely meet the rehabilitation needs of most people's ankles. In the next stage work, the robot hardware structure will be manufactured and the control software will be developed to integrate the ankle rehabilitation robot system in the actual environment. Our future work will focus on control strategies of using the robot for ankle rehabilitation treatment. This will include passive training based on robot pre-defined trajectory tracking control in which robust learning control [24] will be used and the active personalized training based on adaptive impedance control as well as adaptation of robot compliance [25].

REFERENCES

[1] W. Johnson, O. Onuma, M. Owolabi, and S. Sachdev, "Stroke: a global response is needed," ed: World Health Organization, 2016.

[2] C. E. Hiller, E. J. Nightingale, J. Raymond, S. L. Kilbreath, J. Burns, D. A. Black, *et al.*, "Prevalence and impact of chronic musculoskeletal ankle disorders in the community," *Archives of physical medicine and rehabilitation,* vol. 93, pp. 1801-1807, 2012.

[3] D. T.-P. Fong, Y. Hong, L.-K. Chan, P. S.-H. Yung, and K.-M. Chan, "A systematic review on ankle injury and ankle sprain in sports," *Sports medicine,* vol. 37, pp. 73-94, 2007.

[4] S. Shah, A. C. Thomas, J. M. Noone, C. M. Blanchette, and E. A. Wikstrom, "Incidence and cost of ankle sprains in United States emergency departments," *Sports health,* vol. 8, pp. 547-552, 2016.

[5] I. A. Bielska, X. Wang, R. Lee, and A. P. Johnson, "The health economics of ankle and foot sprains and fractures: A systematic review of English-language published papers. Part 1: Overview and critical appraisal," *Foot,* 2017.

[6] W. Petersen, I. V. Rembitzki, A. G. Koppenburg, A. Ellermann, C. Liebau, G. P. Brüggemann, *et al.*, "Treatment of acute ankle ligament injuries: a systematic review," *Archives of orthopaedic and trauma surgery,* vol. 133, pp. 1129-1141, 2013.

[7] W. Meng, Q. Liu, Z. D. Zhou, Q. S. Ai, B. Sheng, and S. Q. Xie, "Recent development of mechanisms and control strategies for robot-assisted lower limb rehabilitation," *Mechatronics,* vol. 31, pp. 132-145, Oct 2015.

[8] M. Zhang, T. C. Davies, and S. Xie, "Effectiveness of robot-assisted therapy on ankle rehabilitation - A systematic review," *Journal of NeuroEngineering and Rehabilitation,* vol. 10, 2013.

[9] K. P. Michmizos, S. Rossi, E. Castelli, P. Cappa, and H. I. Krebs, "Robot-aided neurorehabilitation: a pediatric robot for ankle rehabilitation," *IEEE Transactions on Neural Systems and Rehabilitation Engineering,* vol. 23, pp. 1056-1067, 2015.

[10] K. Bharadwaj, T. G. Sugar, J. B. Koeneman, and E. J. Koeneman, "Design of a robotic gait trainer using spring over muscle actuators for ankle stroke rehabilitation," *Journal of biomechanical engineering,* vol. 127, pp. 1009-1013, 2005.

[11] J. E. Deutsch, J. Latonio, G. C. Burdea, and R. Boian, "Post-stroke rehabilitation with the Rutgers Ankle system: A case study," *Presence: Teleoperators and Virtual Environments,* vol. 10, pp. 416-430, 2001.

[12] J. A. Saglia, N. G. Tsagarakis, J. S. Dai, and D. G. Caldwell, "Control strategies for patient-assisted training using the ankle rehabilitation robot (ARBOT)," *IEEE/ASME Transactions on Mechatronics,* vol. 18, pp. 1799-1808, 2013.

[13] L. N. Awad, J. Bae, K. O'Donnell, D. R. Smm, K. Hendron, L. H. Sloot, *et al.*, "A soft robotic exosuit improves walking in patients after stroke," *Science Translational Medicine,* vol. 9, p. eaai9084, 2017.

[14] J. S. Dai, T. Zhao, and C. Nester, "Sprained ankle physiotherapy based mechanism synthesis and stiffness analysis of a robotic rehabilitation device," *Autonomous Robots,* vol. 16, pp. 207-218, 2004.

[15] J. Huang, X. Tu, and J. He, "Design and evaluation of the RUPERT wearable upper extremity exoskeleton robot for clinical and in-home therapies," *IEEE Transactions on Systems, Man, and Cybernetics: Systems,* vol. 46, pp. 926-935, 2016.

[16] J. Cao, S. Q. Xie, and R. Das, "MIMO Sliding Mode Controller for Gait Exoskeleton Driven by Pneumatic Muscles," *IEEE Transactions on Control Systems Technology,* vol. PP, pp. 1-8, 2017.

[17] Y. H. Tsoi and S. Q. Xie, "Design and Control of a Parallel Robot for Ankle Rehabiltation," *International Journal of Intelligent Systems Technologies & Applications,* vol. 8, pp. 100-113, 2008.

[18] P. K. Jamwal, S. Q. Xie, S. Hussain, and J. G. Parsons, "An adaptive wearable parallel robot for the treatment of ankle injuries," *IEEE/ASME Transactions on Mechatronics,* vol. 19, pp. 64-75, 2014.

[19] P. K. Jamwal, S. Hussain, M. H. Ghayesh, and S. V. Rogozina, "Impedance control of an intrinsically compliant parallel ankle rehabilitation robot," *IEEE Transactions on Industrial Electronics,* vol. 63, pp. 3638-3647, 2016.

[20] M. Zhang, S. Q. Xie, X. Li, G. Zhu, W. Meng, X. Huang, *et al.*, "Adaptive Patient-Cooperative Control of a Compliant Ankle Rehabilitation Robot (CARR) with Enhanced Training Safety," *IEEE Transactions on Industrial Electronics,* 2017.

[21] M. Zhang, B. Sheng, T. C. Davies, W. Meng, and S. Q. Xie, "Model based open-loop posture control of a parallel ankle assessment and rehabilitation robot," in *Advanced Intelligent Mechatronics (AIM), 2015 IEEE International Conference on*, 2015, pp. 1241-1246.

[22] C. G. Mattacola and M. K. Dwyer, "Rehabilitation of the ankle after acute sprain or chronic instability," *Journal of athletic training,* vol. 37, p. 413, 2002.

[23] M. Hiller, S. Fang, S. Mielczarek, R. Verhoeven, and D. Franitza, "Design, analysis and realization of tendon-based parallel manipulators," *Mechanism and Machine Theory,* vol. 40, pp. 429-445, 2005.

[24] W. Meng, S. Q. Xie, Q. Liu, C. Z. Lu, and Q. S. Ai, "Robust Iterative Feedback Tuning Control of a Compliant Rehabilitation Robot for Repetitive Ankle Training," *Ieee-Asme Transactions on Mechatronics,* vol. 22, pp. 173-184, Feb 2017.

[25] Q. Liu, A. M. Liu, W. Meng, Q. S. Ai, and S. Q. Xie, "Hierarchical Compliance Control of a Soft Ankle Rehabilitation Robot Actuated by Pneumatic Muscles," *Frontiers in Neurorobotics,* vol. 11, Dec 2017.